FACTORS CONTROLLING STRESS-RUPTURE OF FIBER-REINFORCED CERAMIC COMPOSITES

J.A. DiCarlo[1] and H.M. Yun[2]

[1,2] *Materials Division, NASA Glenn Research Center, 21000 Brookpark Road Cleveland, OH 44135, USA*

SUMMARY: This paper examines some of the key intrinsic and extrinsic factors that control the stress-rupture behavior of ceramic matrix composites (CMC). Because CMC rupture typically occurs simultaneously with the time-dependent fracture of the ceramic fiber reinforcement, emphasis is placed on elucidating the microstructural, environmental, and physical factors that control the low and high temperature rupture behavior of a variety of oxide and SiC-based fibers. Empirically determined Larson-Miller and Monkman-Grant rupture plots for these fibers are presented and discussed in terms of their basic and practical implications. Using composite theory, mechanical models are developed which show how the fiber data can also be used to understand and predict stress rupture behavior for cracked and uncracked CMC under some simple application conditions. Based on the good agreement observed between the model predictions and CMC results in the literature, some preliminary guidelines are presented for selecting constituents for optimum CMC rupture life.

KEYWORDS: oxide fibers, SiC fibers, rupture, creep, microstructure, oxidation, matrix cracking, rupture models.

INTRODUCTION

The successful application of fiber-reinforced ceramic matrix composites (CMC) depends strongly on maximizing material rupture life over a wide range of temperatures and application conditions. Since the failure of CMC typically occurs simultaneously with the time-dependent fracture of the ceramic reinforcement, the key to maximizing CMC life is the development of an understanding of the many factors that control rupture of individual fibers within a complex CMC environment. This can be a very difficult task since fiber behavior will not only depend on such CMC global variables as stress, temperature, external environment, and their time derivatives, but also on how the fiber experiences these variables on the local level through mechanical, physical, and chemical interactions with the interphase coating, the matrix, and the internal CMC environment.

The objective of this paper is to take an initial step toward understanding the many intrinsic and extrinsic factors that can control the stress rupture behavior of fibers and CMC. This is accomplished first by examining the rupture properties of a variety of continuous-length oxide and SiC-based fibers that are of current interest for CMC reinforcement. These properties were measured using single fibers subjected to simple test conditions intended to simulate a

range of potential CMC application conditions. Emphasis is placed on characterizing fiber performance at high temperatures where CMC have the most technical potential and where the fibers rupture by the creep-controlled growth of strength-limiting flaws. Here the measured fiber rupture properties are analyzed in terms of their basic mechanisms and practical implications. Using composite theory, the single fiber results are then employed to develop simple mechanical models for the rupture behavior of CMC with cracked and uncracked matrices. Although the models apply to simple test conditions, it is shown that the rupture predictions are in good agreement with CMC stress-rupture results in the literature. This offers the opportunity to assess the key factors controlling CMC rupture and to offer some preliminary constituent guidelines for optimizing CMC rupture life for various application conditions.

RESULTS AND DISCUSSION

Fiber Rupture

In previous studies [1-5], the rupture properties of a variety of oxide and SiC-based fibers were measured from 20 to 1400°C under oxidizing (air) and inert (argon) conditions. The measurements were made on single fibers across a time range from ~0.01 to over 100 hours using three types of tests: stress rupture (constant stress and constant temperature), slow warm-up (constant stress, constant rate of temperature change), and fast-fracture (constant temperature and constant rate of stress change). It was found that by simple thermal-activation theory [6,7], the rupture results of the three tests for each fiber type could be combined into a single master curve or q-map which describes the applied stress at rupture (fiber rupture strength) versus the time-temperature dependent parameter **q** given by

$$\mathbf{q \equiv Q_r / 2.3R = T\,(\log t_r + 22)} \qquad (1).$$

Here $\mathbf{Q_r}$ is the effective activation energy for fiber rupture; **R** is the universal gas constant (8.314 J/mol-K); **T** (kelvin) is the absolute temperature for the rupture test; and $\mathbf{t_r}$ (hours) is the fiber rupture time.

Complete q-maps covering a wide range of temperatures and stresses are shown in Fig. 1a for two types of oxide-based fibers: Nextel 610 and Nextel 720, and for two types of SiC-based fibers: Hi-Nicalon and Sylramic. High temperature q-maps are shown in Fig. 1b for four types of SiC-based fibers: Nicalon, Hi-Nicalon, Sylramic, and Ultra SCS. Here the curves represent best-fit averages of the fiber rupture times as measured for a ~25 mm gauge length. Key microstructural properties for the six different fiber types [8] are listed in Table 1. These fibers were selected for this study because their creep and rupture properties span the range that has been observed for ceramic fibers of current interest for high-temperature CMC.

Table 1: Microstructural Properties for As-Produced Fibers Examined in This Study

Fiber Type	Nextel 610	Nextel 720	Nicalon	Hi-Nicalon	Sylramic	Ultra SCS (SCS-X)
Manufacturer	3M	3M	Nippon Carbon	Nippon Carbon	Dow Corning	Textron
Composition	alumina	mullite	SiC	SiC	SiC	SiC
Impurities, ~wt.%	0.3 SiO_2 0.7 Fe_2O_3	48 Al_2O_3	12 O 31 C	0.5 O 36 C	Trace B Trace C	Trace C
Grain Size, nm	~80	~100	~3	~5	~100	~150

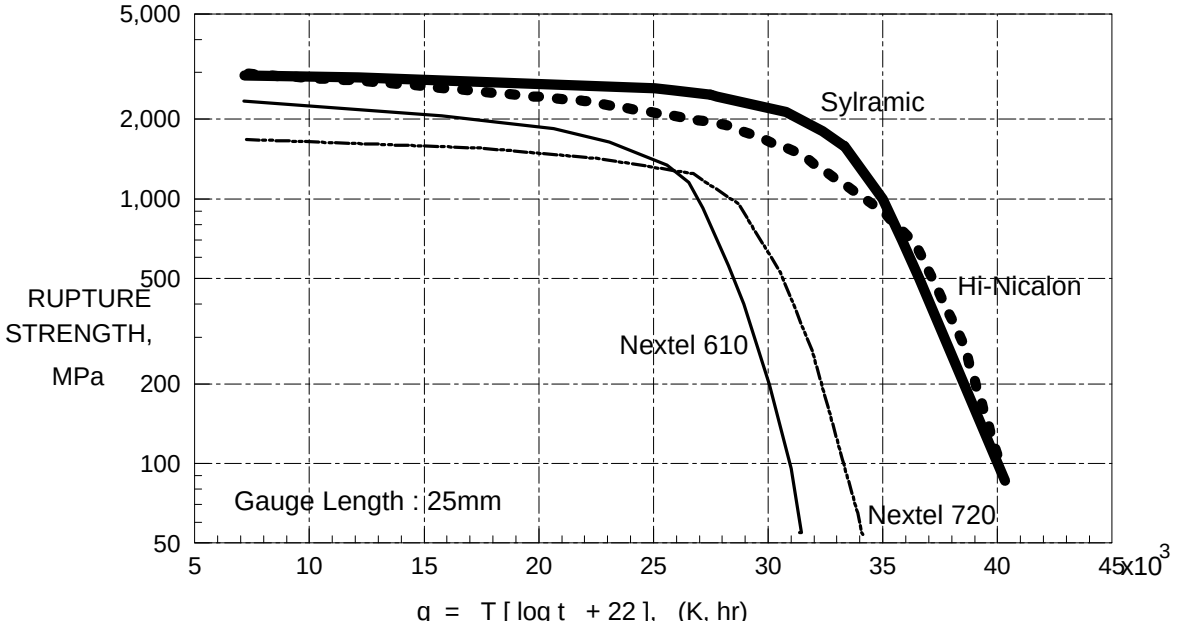

(a)

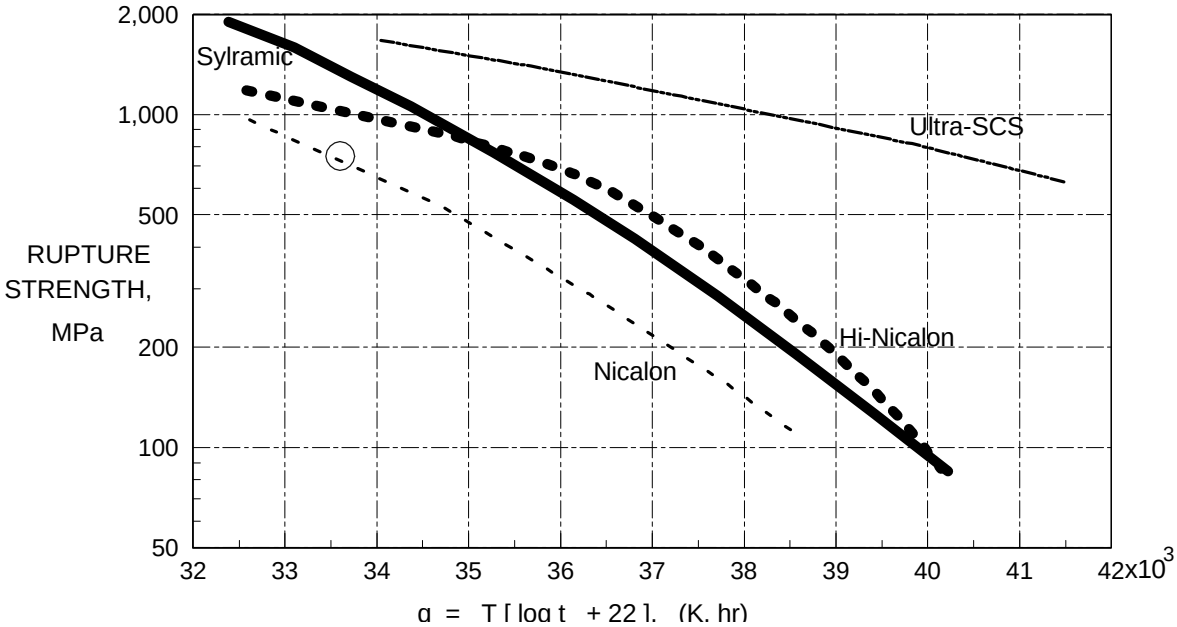

(b)

Fig. 1. Best-fit q-maps or Larson-Miller curves for single fibers in air:(a) oxide and SiC-based fibers in Regions I and II and (b) SiC-based fibers in Region II (open data point is from CMC rupture results in the literature [19]).

The rupture results of Fig. 1a have many important basic and practical implications. First, on the basic level, all curves have the same shape with increasing **q**; that is, an initial section with a small negative slope (Region I), and a remaining section with a much larger negative slope (Region II). This behavior is typical of the rupture of monolithic ceramics in which at low temperatures, as-produced flaws grow slowly in size (slow crack growth); whereas at high temperatures, creep mechanisms aid in the more rapid growth of the same flaws or in the nucleation and growth of new microcracks and cavities [9]. Also, although the curves are essentially the same as empirically-derived Larson-Miller (LM) plots [10], the ability to correlate the parameter q with effective rupture energy (Eqn 1) offers some basic insight not generally realized with the LM approach. For example, the curves show how for high stresses in Region I the rupture activation energy for slow crack growth, $\mathbf{Q_r \equiv 2.3Rq}$, rapidly decreases with increasing stress [11]. In Region II, $\mathbf{Q_r}$ becomes effectively independent of stress as might be expected for flaw growth controlled by a constant creep energy. For Region II, fiber strengths have little dependence on gauge length [2], suggesting a narrow size distribution for the creep-generated flaws.

On the practical side, the Fig. 1 curves indicate that fiber strength values throughout Region I depend directly on the fiber's as-fabricated strength at room temperature (**q** ≈ 7000). That is, the entire Region I section moves up in strength when as-produced flaws are reduced in size or frequency. Alternatively, the section would move up or down if the test gauge length were smaller or greater, respectively, than the ~25 mm length used to generate the curves. In addition, Fig. 1a clearly indicates the greater thermostructural capability of the SiC fibers over the oxide-based fibers both in Regions I and II. As discussed elsewhere [12], the Region I advantage is related to the higher fracture toughness of SiC; while the Region II advantage is primarily due to slower diffusion processes in the SiC-based fibers. Finally, the Fig. 1 curves allow the prediction of fiber rupture behavior if any four of the following five application variables are known: stress, stress rate, temperature, temperature rate, and time [6]. For example, as will be discussed, if the stress on fibers bridging matrix cracks were known, one can then use the single-fiber rupture curves and elementary composite theory to predict the rupture life of cracked CMC for any given application temperature.

One drawback of the Fig. 1 approach is that, as the rupture curves in Region II become steeper and steeper, the q-maps or LM plots begin to lose sensitivity in predicting fiber rupture strength at high temperatures. As mentioned, this is a consequence of the fiber rupture energy becoming equal to the stress-independent fiber creep energy. Also the curves do not allow a direct quantitative assessment of fiber creep resistance. For example, the Hi-Nicalon and Sylramic fibers behave similarly in rupture at the high **q** values, but the Sylramic fiber creeps much less. Since long rupture time and high creep resistance are both desirable fiber properties for CMC performance, the fiber creep-rupture data were also analyzed in terms of Monkman-Grant (MG) diagrams which plot the log of fiber rupture time versus the log of fiber creep rate at various temperatures [13]. On MG diagrams, the log-log results at various temperatures typically fall on a set of parallel straight lines [14,15].

Fig. 2a shows the best-fit MG lines in air for log of average rupture time (hours) versus log of steady state creep rate (sec^{-1}) for the Nextel 610 fiber at 980 and 1090^{o}C and for the Nextel 720 fiber at 1090^{o}C. The solid segment on each line represents the rupture data measured between ~100 MPa and 500 MPa (O). This stress range is considered typical for fibers within structural CMC. The fibers displayed steady state creep from nearly initial loading to rupture; so that average rupture strain can be determined by simply multiplying rupture time by creep rate. In support of a weak temperature effect, Fig. 2a shows that the Nextel 610 lines fall very closely to the hashed area which is the range of MG lines measured at 1150 and

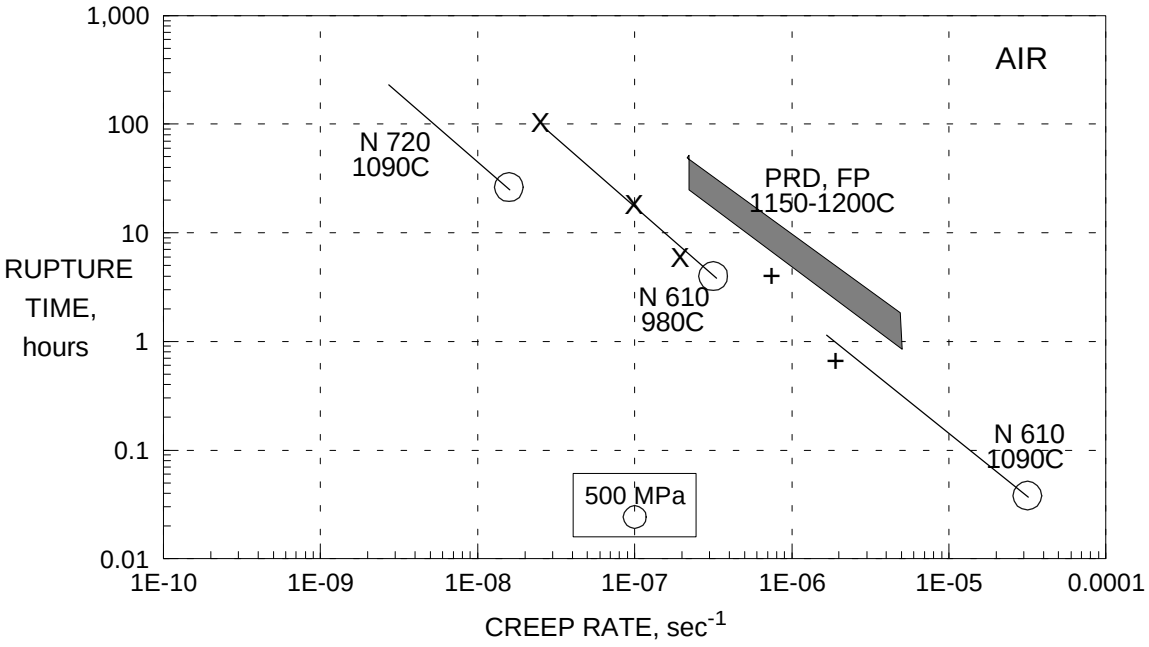

(a)

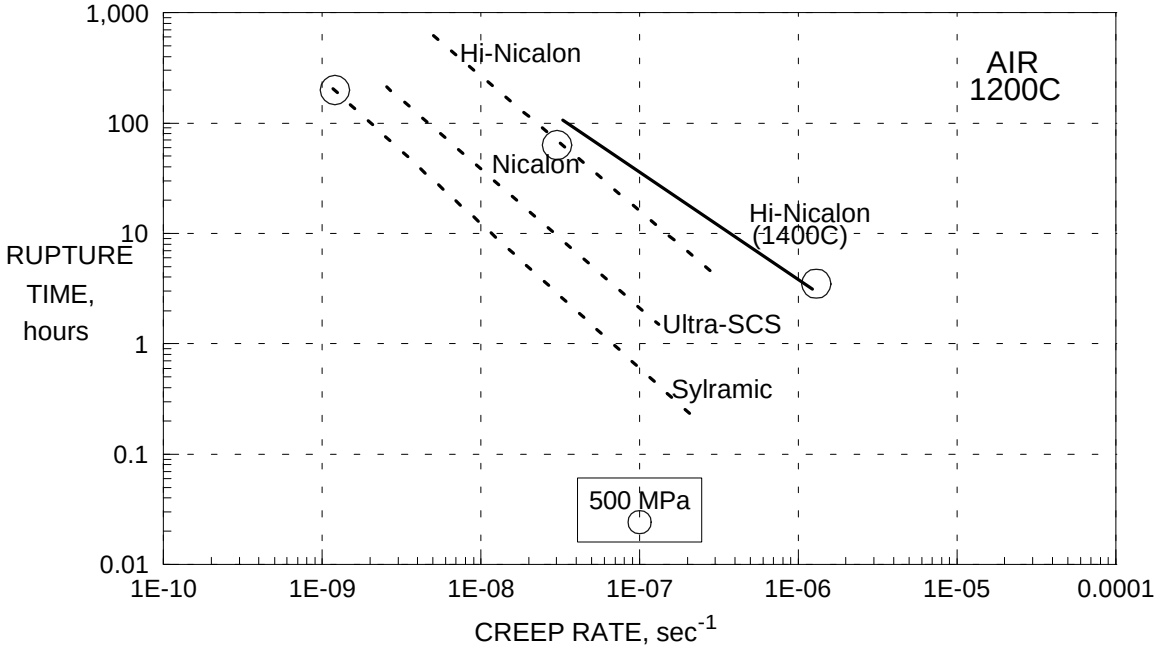

(b)

Fig. 2. Best-fit Monkman-Grant lines in air for (a) oxide-based single fibers from 980 to 1200°C (data points are Nextel 610 CMC rupture results at 1000°C (X) and 1100°C (+)[20]) and (b) SiC-based single fibers at 1200°C and the Hi-Nicalon fiber at 1400°C.

1200°C for two other alumina-based fibers, FP and PRD-166 [14]. Thus, for a given temperature and creep rate, all the alumina-based fibers appear to rupture within a very narrow distribution of times. Also to be noted is that the MG line for the more creep-resistant mullite-based Nextel 720 fiber is below the extrapolated range for the alumina fibers, displaying about an order of magnitude smaller rupture time and strain at the same creep rate.

Regarding MG plots for the SiC-based fibers, all types displayed a large transient creep stage with rupture typically occurring in this stage. For this reason there was no creep stage that could reliably be labeled as steady state. Nevertheless, as is often the case with monolithic ceramics [15], fairly consistent MG plots can still be constructed based on the minimum creep rate. Using this approach, Fig. 2b shows the best-fit lines for average rupture time versus minimum creep rate (or instantaneous rate at rupture) for the four SiC types at 1200°C in air. To show the general effect of test temperature, Fig. 2b also includes MG results for the Hi-Nicalon fiber tested at 1400°C in air. Dashed and solid MG lines are used to represent, respectively, data measured above and below ~500 MPa (O).

There are many interesting observations that can be made from MG results of Fig. 2b. For example, the rupture times of the SiC-based fibers at 1200°C in air displayed a larger distribution than that of the alumina-based fibers. This may be due to the large amount of excess carbon in the Nicalon and Hi-Nicalon fibers (cf. Table 1). However, at the same temperature and creep rate, the SiC and oxide distributions overlap to a great degree. On the basic level, this indicates that under these conditions, the rupture strains of all the fibers fall within a narrow range and are thus weakly dependent on the Table 1 microstructural factors. Therefore fiber rupture time is strongly dependent on fiber deformation rate, which may be internally or externally controlled. On the practical level, it would appear then that for a particular application temperature, one cannot select fiber rupture time independently of fiber creep rate. For example, Fig. 2 indicates that up to 1200°C, the only approach for obtaining a 1000-hour fiber lifetime is to assure that the CMC application conditions do not create fiber creep rates more than ~10^{-8} sec^{-1} for the creep–prone fibers (Nextel 610 and Hi-Nicalon) and more than ~10^{-9} sec^{-1} for the creep–resistant fibers (Nextel 720 and Sylramic).

Finally, the MG lines of Fig. 2 can be described by the following empirical equation:

$$\mathbf{t_r\, \acute{e}^m = C} \qquad (2).$$

Here $\mathbf{t_r}$ is the average rupture time, **é** is the steady state (or minimum) creep rate, and **m** and **C** are empirical parameters that are weakly dependent on temperature. It is interesting to note that between 1000 and 1200°C, all the fiber types displayed about the same **m** value of ~1.2. The fact that the exponent **m** is greater than unity indicates that the average fiber rupture strain ($\approx$ **é** $\mathbf{t_r}$) increased with increasing rupture time or decreasing creep rate. However, the oxide fibers displayed slightly higher **C** values than the SiC-based fibers at the same test temperature. This supports the general observation in Fig. 2 that at a given creep rate, the more creep-prone fibers will display longer rupture times and higher rupture strains than the more creep resistant fibers. It should also be noted that at 1400°C in air, the Hi-Nicalon fiber and the Sylramic fiber (not shown) were observed to display **m** values less than unity, implying reduced rupture strain with longer rupture time. This effect may be related to detrimental effects associated with microstructural changes or with long-term oxidation. However, at 1400°C in argon, the rupture strains of these fibers were ~50% smaller than in air [5]. This improved behavior in air, which was also observed for other small-diameter SiC fibers, appears to be related to silica growth on the fiber surface. Apparently the formation of a thin silica layer inhibits growth of the surface flaws that eventually cause fiber rupture.

CMC Rupture

The single fiber results presented above indicate that many intrinsic and extrinsic factors control rupture of fiber types of current interest for CMC reinforcement. As an initial step toward understanding the relative importance of each of these factors, the following discussion assumes some simple CMC application conditions and uses elementary composite theory and the single fiber data to develop predictive models for CMC rupture. These predictions are then compared with CMC stress rupture results in the literature to show good agreement, at least under simple test conditions. This analysis in turn is used to shed some light on the key factors controlling rupture of CMC with cracked and uncracked matrices.

One very important CMC application condition is that in which the composite contains through-thickness matrix cracks that are bridged by the fiber reinforcement. These cracks could have developed during CMC fabrication due to a thermal expansion mismatch between the fibers and matrix, or during CMC service due to some random overstress or the need for a high design stress. For a simple rupture model, one might assume that the application requires the cracked CMC to experience a relatively constant uniaxial stress σ_c at a constant temperature **T** in an air environment. If V_f^* is the effective fiber volume fraction bridging the through-thickness cracks in the stress direction, ultimate fracture or rupture of the CMC should then occur at time t_r when the following stress condition is satisfied:

$$\sigma_c = \sigma_c^r = V_f^* \, \sigma_B^r (t_r, T, L_e) \qquad (3).$$

Here σ_c^r is the CMC rupture strength, σ_B^r is the average rupture strength of the fiber bundles within the cracks, and L_e is the effective bundle gauge length within the cracks. Curtin [16] has shown that when interfacial conditions and bundle fracture statistics are taken into account, a good approximation for $\sigma_B^r(L_e)$ at room temperature is the average strength of individual fibers measured at ~25 mm gauge length. Assuming this is the case at all temperatures, CMC rupture strengths should then be predictable from the following relation:

$$\sigma_c^r \approx V_f^* \, \sigma_f^r (q, 25 \text{ mm}) \qquad (4).$$

Here $\sigma_f^r(q, 25 \text{ mm})$ can be directly determined from the LM curves of Fig. 1.

Although the assumptions used for the Eqn 4 model are very simple and perhaps unrealistic for many CMC applications, they do closely simulate typical test conditions that have been used to study the creep and rupture properties of CMC [17]. For example, Morscher [18] has evaluated the effects of pre-cracked matrices on the stress-rupture behavior of one-dimensional SiC/SiC minicomposites containing Hi-Nicalon multifilament tows, BN interphases, and SiC matrices that were produced by chemical vapor infiltration (CVI). Under ambient air conditions in both Regions I and II, he found that the Fig. 1 curves for the Hi-Nicalon fiber gave very good predictions of the CMC rupture times as long as the interfacial conditions were sufficient to allow the fibers to fracture independently (global load sharing). Attack of the BN interphases by the ambient air occurred above 500^{o}C, resulting in its removal and replacement by borosilicate glass with increasing time and temperature. This glass resulted in strong fiber-matrix bonds so that CMC strengths were less than optimum for high applied stresses from ~900 to 1100^{o}C (**q** values from ~27000 to 33000). At higher temperatures and lower stresses, the glass bonds were apparently compliant enough so that under stress-rupture conditions, the fibers were able to act independently, again giving good agreement with the single fiber LM curves. These minicomposite results not only show the usefulness of Fig. 1 and Eqn 4 for predicting the optimum stress-rupture behavior of CMC

with through-thickness matrix cracks, but also indicate the important degradation effects that can occur when SiC-based fibers and current interphases are exposed to oxidizing conditions.

Besides minicomposites, high temperature stress-rupture data also exist in the literature for woven two-dimensional SiC/SiC. For example, Zhu et al [19] recently performed creep and rupture studies at various stresses at 1300°C in air on CMC with Nicalon fibers, carbon interphases, and CVI SiC matrices enhanced by boron-containing additives. Taking the rupture time at the highest CMC stress (150 MPa) where the matrix was presumably cracked, one can then employ Eqn 1 and Eqn 4 with $\mathbf{V_f^*} \approx 20\%$ to calculate the rupture strength at a given **q** value for the Nicalon fiber bundles bridging the matrix cracks. The open data point in Fig. 1b shows the calculated bundle strength. The good agreement with the LM curve for single Nicalon fibers further supports the assumptions of the Eqn-4 rupture model, even for CMC with complex fiber architectures. It also supports the observation of Zhu et al that interior carbon interphases were retained due to crack sealing by borosilicate glass formation.

At some low CMC stress in Region II, it is to be expected that the matrix will not crack during stress application so that the CMC load is shared in a time-dependent manner by the fibers and matrix. Since the fibers are not carrying the full CMC load, Eqn 4 and the LM curves of Fig. 1 would underestimate fiber rupture time. To cover this situation, the following model is proposed for the rupture life of uncracked CMC; that is, CMC in which the matrix carries some portion of the composite load. Assuming the fiber and matrix experience the same axial strain (isostrain conditions), the initial creep rate of an uncracked CMC will generally be controlled by the creep-prone constituent and the final creep rate by the creep-resistant constituent [17]. If near steady-state conditions are reached in the CMC life, it is proposed that the minimum CMC creep rate and the MG lines of Fig. 2 could then be used to predict fiber and CMC rupture time. In support of this approach, Zuiker [20] has recently analyzed the creep and rupture behavior of a woven oxide/oxide CMC reinforced by Nextel 610 fibers. At 1000 and 1100°C in air, after a rapid transient stage due to some amount of matrix stress relaxation, these CMC showed a long steady-state creep stage prior to rupture. If one plots the CMC rupture time versus the CMC creep rate, one obtains the data points (×,+) shown in the MG plot of Fig. 2a. It can be seen that these points are in excellent agreement with the solid lines for the Nextel 610 fiber measured at nearly the same temperatures.

Mathematically, one can describe the proposed rupture model for uncracked CMC as follows:

$$\mathbf{t_r = C / \dot{\varepsilon}_c^{\,m}} \qquad (5).$$

Here $\mathbf{t_r}$ is the CMC rupture life, $\mathbf{\dot{\varepsilon}_c}$ is the minimum CMC creep rate, and **m** and **C** are the best-fit MG parameters as determined by fitting Eqn 2 to the Fig. 2 line for the reinforcing fiber. Eqn 5 suggests that for long CMC life, fiber and matrix creep rates should be as low as possible in order to minimize the CMC creep rate. However, if the matrix should control the CMC creep rate, the more creep-prone fibers with the higher **C** values should allow a longer CMC life, provided the matrix does not crack first. In this regard, it is interesting to assume that SiC matrices produced by CVI will creep and rupture in a manner equivalent to that of the Ultra SCS fiber which is produced by chemical vapor deposition. One might then examine Fig. 2b to suggest that at 1200°C the Sylramic fibers will rupture before the CVI SiC matrix cracks; while the Nicalon and Hi-Nicalon fibers will probably rupture very soon after matrix cracking. Clearly more work is needed in this area since practical situations can exist where CMC stresses are low enough to avoid initial matrix cracking, but high enough to cause composite creep.

SUMMARY AND CONCLUSIONS

This paper has shown that single fiber data measured on various oxide and SiC-based fiber types can be used not only to understand the various factors controlling fiber rupture, but also to predict with reasonable accuracy when CMC will rupture for some simple application conditions. Accordingly, one should now be able to develop some preliminary guidelines for selecting CMC constituents that will maximize CMC rupture behavior. For example, for time-temperature conditions in Region I, the key factors controlling fiber rupture are the as-produced flaw sizes and the fiber composition. These together determine the room temperature strength of the fiber and its time/temperature-dependent rate of degradation due to slow crack growth. In this regard, the SiC-based fibers typically behave better than oxide fibers due to their higher toughness. However, at the stress levels required to utilize this strength advantage, CMC matrices will be cracked and the fibers and interphases will be exposed to the application environment. For oxidizing conditions and temperatures above ~500^{o}C, the interphases currently being used on the SiC-based fibers will typically disappear, allowing the oxidation-prone SiC fibers to bond with each other and with the matrix in a complex manner. Thus full advantage of the SiC-based fibers cannot be taken in Region I unless more durable interphases are developed.

For stress rupture conditions and cracked matrices in Region II, there does not appear to be as strong a need for oxidation-resistant interphases if the matrix is silicon-based and contains boron additives. Apparently because fiber rupture strengths are low in Region II, CMC stresses and matrix crack openings are small, thereby allowing crack sealing by formation of borosilicate glass. Under these conditions, the Larson-Miller plots presented here clearly show that SiC-based fibers should display longer rupture times than the oxide-based fibers. However, it is also shown that there still can be important differences in creep rates, rupture times, and rupture strains for the various SiC fiber types. For example, for a given stress, the Sylramic fiber is more creep-resistant than the Hi-Nicalon fiber, but does not show any improvement in rupture time because of a much lower rupture strain. As discussed here, these differences could become important for CMC applications in which the matrix is uncracked and more creep resistant than the fibers. Thus although the SiC-based fibers are generally preferred for Region II, fiber type selection for optimum CMC life may depend on a variety of complex factors, including those not usually considered, such as whether the matrix will carry load or not during CMC life.

Finally, a CMC rupture model was presented here that uses single fiber Larson-Miller results to closely predict CMC rupture time for simple application conditions in which the matrix is cracked (or fully relaxed) and the fibers are able to act independently throughout CMC life. If these microstructural conditions are not met, the model predictions can still serve as a guideline to understand the underlying mechanisms controlling CMC rupture. For example, if measured CMC strengths were less than predicted, one might conclude that the loss of fiber independence occurred, for example, by interphase attack. On the other hand, if measured CMC strengths were greater than predicted, one might conclude that the matrices did not crack and were still able to carry some portion of the CMC load. For this latter situation, it is suggested here that the single-fiber Monkman-Grant results could then be used to predict fiber and CMC rupture. Thus simple measurements on single fibers can provide not only a base for CMC life optimization, but also for CMC rupture analysis.

REFERENCES

1. Yun, H.M., Goldsby, J.C., and DiCarlo, J.A., "Time-Temperature Effects on the Rupture and Creep Strength of Oxide Fibers", to be published.
2. Yun, H.M., Goldsby, J.C., and DiCarlo, J.A., "Tensile Creep and Stress-Rupture Behavior of Polymer Derived SiC Fibers", *Ceramic Transactions*, Vol. 46, 1994, pp. 17-28.
3. DiCarlo, J.A., Yun, H.M., and Goldsby, J.C., "Creep and Rupture Behavior of Advanced SiC Fibers", *Proceedings of ICCM-10*, 1995, Vol. VI: Microstructure, Degradation, and Design, Poursartip, A. and Street, K.N., Eds, pp. 315-322.
4. Yun, H.M., Goldsby, J.C., and DiCarlo, J.A., "Thermomechanical Behavior of Three Types of CVD SiC Monofilaments", *HiTEMP Review 1995*, Vol. III, NASA Conference Publication 10178, 1995, paper 56.
5. Yun, H.M., Goldsby, J.C., and DiCarlo, J.A., "Environmental Effects on Creep and Stress-Rupture Properties of Advanced SiC Fibers", *Proceedings For HTCMC-2, II*, Evans, A.G. and Naslain, R., Eds., *Ceramic Transactions*, Vol. 57, 1995, pp. 331-336.
6. Yun, H.M. and DiCarlo, J.A., "Time/Temperature Dependent Tensile Strength of SiC and Al_2O_3-Based Fibers", *Ceramic Transactions*, Vol. 74. 1996, pp. 17-26.
7. DiCarlo, J.A. and Yun, H.M., "Thermostructural Performance Maps for Ceramic Fibers", *Proceedings of CIMTEC '98*, Florence, Italy, 1998.
8. DiCarlo, J.A. and Dutta, S., "Continuous Ceramic Fibers for Ceramic Composites", *Handbook On Continuous Fiber Reinforced Ceramic Matrix Composites*. Lehman,R., El-Rahaiby, S., and Wachtman, Jr., J., Eds., CIAC, Purdue University, West Lafayette, Indiana, 1995. pp 137-183.
9. Evans, A.G. and Blumenthal, W., "High Temperature Failure in Ceramics", *Fracture Mechanics of Ceramics*, Vol. 6, Measurements, Transformations, and High-Temperature Fracture, Bradt, R.C., Evans, A.G., Hasselman, D.P.H., and Lange, F.F., Eds., Plenum Press, New York, 1973, pp. 423-448.
10. Larson, F.R. and Miller, J., "A Time-Temperature Relationship for Rupture and Creep Stresses", *Trans. ASME*, Vol. 74, 1952, pp. 765-775.
11. Gupta, P.K., "Relation Between Power and Exponential Laws of Slow Crack Growth", *Commun. Am. Ceram. Soc*., Vol. 65, No. 10, 1982, pp. C-163 164.
12. DiCarlo, J.A. and Yun, H.M., "Microstructural Factors Affecting Creep-Rupture Failure of Ceramic Fibers", *Ceramic Transactions*, Vol. 99, 1998, pp. 119-134.
13. Monkman, F.C. and Grant, N.J., "An Empirical Relationship between Rupture Life and Minimum Creep Rate", *Proc. ASTM*, Vol. 56, 1956, pp. 593-620.
14. Pysher, D.J. and Tressler, R.E., "Tensile Creep Rupture Behavior of Alumina-Based Polycrystalline Oxide Fibers", *Ceram. Eng. Sci. Proc*., Vol. 13, No. 7-8, 1992, pp. 218-226.
15. Weiderhorn, S.M., Hockey, B.J., Krause, Jr., R.F., and Jakus, K., "Creep and Fracture of a Vitreous-Bonded Aluminum Oxide", *J. of Mat. Sci*., Vol. 21, 1986, pp. 810-824.
16. Curtin, W.A., "Ultimate Strengths of Fibre-Reinforced Ceramics and Metals", *Composites*, Vol. 24, 1993, pp. 98-102.
17. Holmes, J.W. and Wu, X., "Elevated Temperature Creep Behavior of Continuous Fiber-Reinforced Ceramics", *High Temperature Mechanical Behavior of Ceramic Composites*, Nair, S. and Jakus, K., Eds., Butterworth-Heinemann, Newton, MA, 1995, pp.193-259.
18. Morscher, G.N., "Tensile Stress Rupture of SiC/SiC Minicomposites with Carbon and Boron Nitride Interphases at Elevated Temperatures in Air", *J. Am. Ceram. Soc*, Vol. 80, No. 8, 1997, pp. 2029-2042.
19. Zhu, S., Mizuno, M., Nagano, Y., Cao, J., Kagawa, Y., and Kaya, H., "Creep and Fatigue Behavior in an Enhanced SiC/SiC Composite at High Temperature", *J. Am. Ceram. Soc*., Vol. 81, No. 9, 1998, pp. 2269-2277.
20. Zuiker, J.R. "A Model for the Creep Response of Oxide-Oxide Ceramic Matrix Composites", *Thermal and Mechanical Test Methods and Behavior of Continuous-Fiber Ceramic Composites*, ASTM STP 1309, Jenkins, M., Gonczy, S., Lara-Curzio, E., Ashbaugh, N., and Zawada, L.,Eds., American Society for Testing and Materials, 1997, pp. 250-263.